ST-ECF Instrument Science Report WFC3-2008-16

The TV3 ground calibrations of the WFC3 NIR grisms

H. Kuntschner, H. Bushouse, J. R. Walsh, M. Kümmel
July 10, 2008

ABSTRACT

Based on thermal vacuum tests (TV3; March/April 2008), the performance of the WFC3 near-IR G102 and G141 grisms together with the new IR detector (IR4; FPA165) has been assessed. In this ISR we report on the new throughput measurements for both grisms and show that the current trace and dispersion solutions are consistent with the ones established during TV2. Furthermore, a new flat-field cube is determined.

1. Introduction

The Wide Field Camera 3 (WFC3) recently underwent the third ground testing in thermal vacuum (TV) conditions. A new IR detector (IR4; FPA165) is now installed in the instrument, re-placing the detector used during the 2007 TV tests (IR1; FPA129). In this ISR we determine new throughput measurements for the NIR channel with two grisms, G102 and G141, for the shorter (800 - 1150nm) and longer NIR wavelengths (1100-1700nm), respectively.

This instrument science report (ISR) is a follow up on the report by Kuntschner, Bushouse, Walsh & Kümmel (WFC3-2008-15) of the TV2 calibrations. The calibration set-up and instrument configuration was similar to the one used in TV2. However, only a restricted set of calibrations and wavelength steps was carried out to establish primarily the new throughput measurements.

2. Calibration measurements

For each IR grism calibration measurements were carried out to allow determination of the spectral trace, the dispersion solution and the absolute instrument throughput as well as a wavelength dependent flat-field. A summary of all NIR grism calibration procedures is given in Table 1. In TV3 absolute throughput, trace and dispersion calibrations are measured only for a central position in the IR channel field of view. In TV2 the trace/dispersion solutions were carried out in a 5-point pattern covering the FoV (Kuntschner et al. 2008).

Table 1. Summary of NIR grism calibrations during TV3

Test procedure	Date	Grism	Purpose
IR14S01	**2008-03-14/17/18**	**G102**	**Flat field**
IR14S02	**2008-03-14/17**	**G141**	**Flat field**
IR14S03	**2008-03-16**	**G102**	**Absolute throughput**
IR14S04	**2008-03-16**	**G141**	**Absolute throughput**
IR16S10	**2008-04-06**	**G102**	**Trace/Dispersion (center)**
IR16S60	**2008-04-06**	**G141**	**Trace/Dispersion (center)**

The absolute throughput measurements were carried out with a calibrated monochromator source covering for the G102 grism the range 780nm - 1180nm in steps of 20nm; and for the G141 grism the range 1040nm – 1700nm in steps of 20nm. For the G102 the trace and dispersion calibrations were carried out starting with a set of three direct image - grism pairs using a white light stimulus. After that monochromator steps covering the range 760nm - 1180nm in steps of 20nm were performed. For the G141 grism, only one pair of direct image and grism image with white light stimulus was carried out at the beginning of the sequence. Furthermore a reduced number of monochromator wavelength settings in the range 1100nm – 1590nm in steps of 70nm was carried out. In all cases, the monochromator bandwidth was 10 nm.

Additionally, the detector flat-field was determined with 10nm wide bandpasses in steps of 20nm, covering for the G102 grism the range 800nm - 1180nm; and for the G141 grism the range 1060nm – 1700nm. For each grism there are two sets of flat-field calibration available.

3. Analysis

In this section we describe the analysis of the TV3 calibration data yielding the confirmation of existing trace and wavelength calibrations and presenting updated throughput measurements and flat-field cubes.

3.1. Trace calibration

The installation of the new IR detector will have a significant effect on the throughput measurements (see Section 3.3), however, it is expected that the main trace and dispersion characteristics, which are determined by the unchanged grisms, remain stable. Hence only one central pointing was observed for the trace and wavelength calibrations during TV3. The trace and wavelength calibration for science data will need to be carried out in orbit with astronomical standard sources (such as flux standard stars and PNe); here in this report we only check for consistency of the solutions derived from TV2 data with the TV3 observations.

The analysis was carried out in the same manner as described for TV2 (see Kuntschner et al. 2008) and no differences were found in terms of trace quality and linearity of the traces. The trace definitions are of the form $(Y-Y_{ref})$=DYDX_0 + DYDX_1*$(X-X_{ref})$. In Table 2 we compare the values derived from TV3 data with the predictions based on the field dependent TV2 solutions. We find good agreement between the field dependent solution derived from TV2 calibrations and the central measurement taken during TV3. Specifically, the zero points of the linear trace agree to better than 0.1 pixel and the slope agrees to 0.2 pixel over 100 pixel in x.

We conclude that the 1st order trace determined during TV3 for one central position is consistent with the field-dependent solution derived from TV2 calibrations. This confirms that the installation and alignment of the new IR detector within the WFC3 optical train has not resulted in any significant change with respect to the geometrical alignment with the grisms.

Table 2: Comparison of 1st order linear trace solutions between TV2 and TV3 for one central position

	Xref [pix]	Yref [pix]	DYDX_0	DYDX_1
G102:				
TV3	349.52	462.23	-1.27	0.013
TV2 prediction			-1.25	0.011
G141:				
TV3	348.74	552.57	0.85	0.009
TV2 prediction			0.95	0.008

3.2. Wavelength solutions

The trace definitions derived from the TV2 analysis were used to extract the monochromator spectra with the standard aXe task AXECORE. The FITS files produced by aXe were then analyzed by custom built IDL scripts where the location of the peak of each monochromator spot was measured by fitting a Gaussian.

The wavelength solutions were found to be well approximated by linear fits to wavelength versus pixel offset. In Table 3 we compare the values derived from TV3 data with the predictions based on the field dependent TV2 solutions.

We find good agreement between the field dependent solution derived from TV2 calibrations and the central measurement taken during TV3. Specifically, the wavelength zero points agree to within 0.25 pixel (or 6 Å) and the dispersion is consistent to within 0.1 Å.

We conclude that the 1st order wavelength solution determined during TV3 for one central position is consistent with the field-dependent solution derived from TV2 calibrations.

Table 3: Comparison of 1st order wavelength solutions between TV2 and TV3 for one central position

	Xref [pix]	Yref [pix]	DLDP_A_0 [Å]	DLDP_A_1 [Å/pix]
G102:				
TV3	349.52	462.23	6371.9	24.52
TV2 prediction			6377.6	24.56
G141:				
TV3	348.74	552.57	8950.4	46.70
TV2 prediction			8954.0	46.80

3.3. Absolute throughput calibrations

For each of the calibrated monochromator settings (see also Section 2) and all visible orders, the detected counts were measured with the IRAF task imexam. The aperture radius was adjusted with 3 iterations, generally resulting in radii of about 17 pixel. The ratio of detected flux (using an effective gain of 2.26 e/DN[1]) versus the incoming flux as recorded in the image headers (keyword OSFLUX, given as flux per second) gives then the instrument efficiency. Figures 4 and 5 present the efficiency curves for WFC3 with the G102 and G141 grisms, respectively. The plots show the efficiency of WFC3 as measured in TV3 but do not include any contributions from the OTA throughput.

For G102, the peak efficiency of ~50% is reached between 1020 and 1120nm in the +1st order. Efficiency above 10% is achieved over a broad wavelength range from 800 to 1140nm. Due to the excellent design of the grism, the throughput in the +2nd and zeroth order is much lower with a maximum of 7% and 2%, respectively. The mean, relative increase in efficiency of the first order between TV3 and TV2 measurements is ~60%. The relative efficiency increase ranges from 67% in the blue to 52% in the red for G102, which is due to the increased QE of the new IR detector.

[1] The effective gain is defined here as the product of the traditional gain value of 2.60 e/DN and the Intra-Capacitance (IPC) correction of 0.87.

For G141, the peak efficiency of ~55% is reached between 1400 and 1600nm in the +1st order. Efficiency above 10% is achieved over a broad wavelength range from 1080 to 1680nm, thus giving continuous wavelength coverage from 800 to 1680nm with the two grisms together. Due to the excellent design of the G141 grism, the throughput in the +2nd, 3rd and zeroth order is much low with a maximum of 10, 1 and 2%, respectively. The mean, relative increase in efficiency of the first order between TV3 and TV2 measurements is ~45%. The relative efficiency increase ranges from 70% in the blue to 21% in the red for G141.

Tables 6 and 7 present the efficiency measurements in tabular form for the G102 and G141 grisms, respectively.

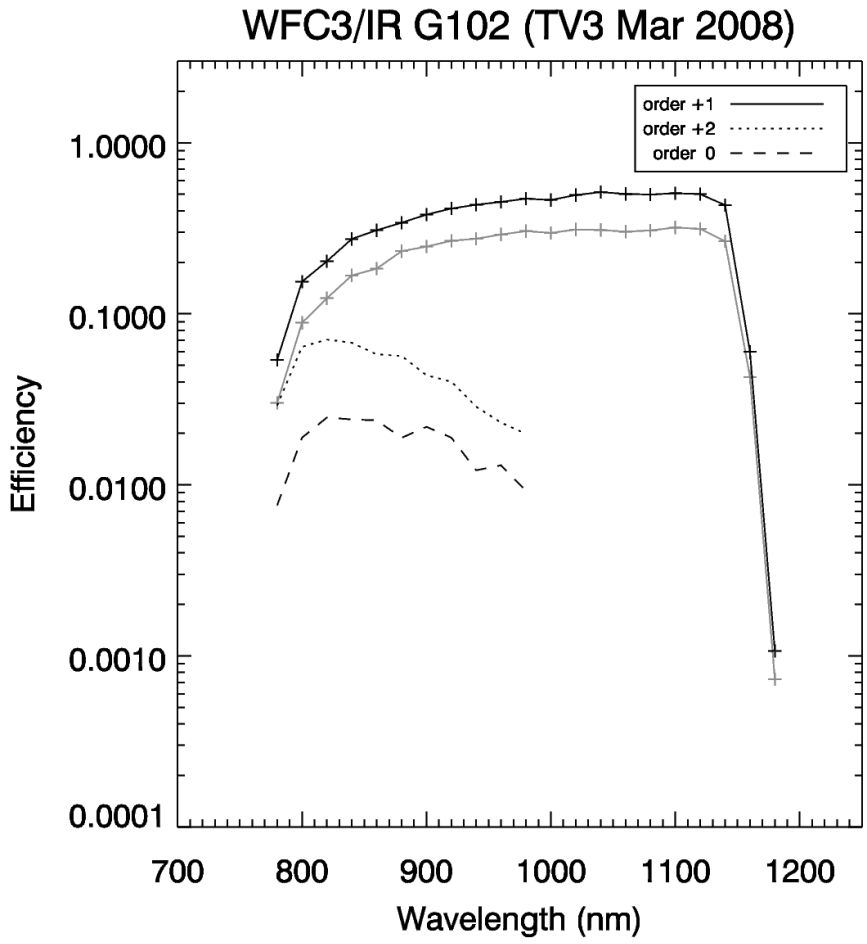

Figure 1: Instrument efficiency of various orders for the WFC3 G102 grism as function of wavelength. For comparison the grey line shows the efficiency of the first order derived during TV2 with the previous NIR detector.

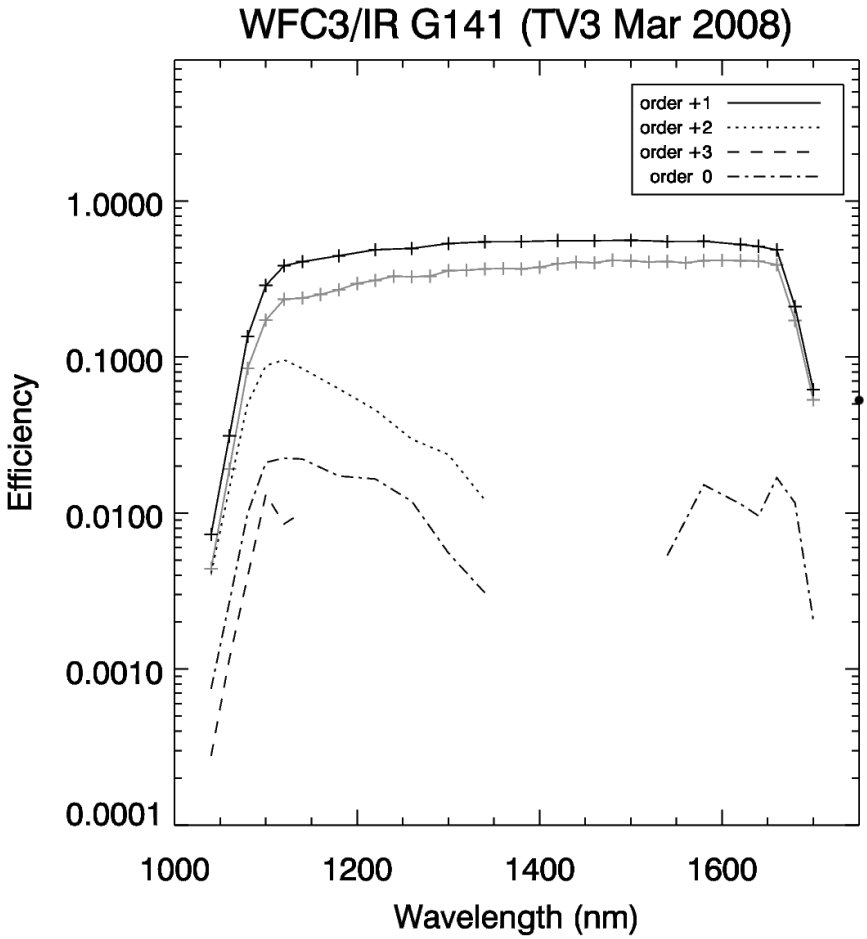

Figure 2: Instrument efficiency of various orders for the WFC3 G141 grism as function of wavelength. The wavelength coverage is interrupted for 0^{th} order on account of insufficient signal. For comparison the grey line shows the efficiency of the first order derived during TV2 with the previous NIR detector.

Table 3: Instrument efficiency for WFC3 G102 (based on TV3)

Wavelength (nm)	0th order	1st order	2nd order
7800	0.0076	0.0537	0.0291
8000	0.0189	0.1539	0.0641
8200	0.0248	0.2029	0.0707
8400	0.0241	0.2738	0.0677
8600	0.0238	0.3078	0.0579
8800	0.0188	0.3405	0.0568
9000	0.0218	0.3801	0.0437
9200	0.0189	0.4123	0.0400
9400	0.0122	0.4341	0.0286
9600	0.0130	0.4506	0.0231
9800	0.0092	0.4709	0.0199
10000	-	0.4625	-
10200	-	0.4941	-
10400	-	0.5145	-
10600	-	0.5022	-
10800	-	0.4976	-
11000	-	0.5067	-
11200	-	0.5008	-
11400	-	0.4318	-
11600	-	0.0598	-
11800	-	0.0011	-

Table 4: Instrument efficiency for WFC3 G141 (based on TV3)

Wavelength (nm)	0th order	1st order	2nd order	3rdorder
10400	0.0007	0.0073	0.0041	0.0003
10600	0.0027	0.0312	0.0144	0.0012
10800	0.0099	0.1352	0.0504	0.0039
11000	0.0211	0.2872	0.0881	0.0132
11200	0.0225	0.3844	0.0958	0.0085
11400	0.0222	0.4082	0.0844	0.0101
11800	0.0173	0.4454	0.0625	-
12200	0.0165	0.4871	0.0458	-
12600	0.0119	0.4962	0.0297	-
13000	0.0056	0.5335	0.0237	-
13400	0.0031	0.5470	0.0121	-
13800	-	0.5487	-	-
14200	-	0.5569	-	-
14600	-	0.5556	-	-
15000	-	0.5598	-	-
15400	0.0053	0.5502	-	-
15800	0.0152	0.5525	-	-
16200	0.0114	0.5255	-	-
16400	0.0096	0.5118	-	-
16600	0.0168	0.4853	-	-
16800	0.0116	0.2102	-	-
17000	0.0021	0.0617	-	-

3.4. Flat-field determinations

An identical procedure for producing monochromatic flat-fields was followed as for TV2 (see Kuntschner et al. 2008). Using CASTLE and the monochromator the G102 and G141 grisms were illuminated with light over the wavelength range of each grism: for G102 8000 to 11800Å in steps of 200Å; for G141 10600 to 17000Å, also in steps of 200Å. The monochromator slit was set to produce light of wavelength width 100Å.

Figure 3 shows the G102 image at 10000 Å. The illumination pattern was removed by fitting a surface using the IRAF task **imsurfit** as for TV2. Figure 4 shows the resulting normalized flat-field for G102 at 10000Å. There is a circular dark region (~40 pixel diameter) at the bottom of the detector, which corresponds to a region of dead pixels. A further notable feature of reduced detector sensitivity is placed towards the lower right of the detector. Only the G102 flat is shown here; the G141

flat-field images are very similar in appearance. The sets of flat-fields were fitted pixel-by-pixel with wavelength as for TV2, and the residual images on the fit showed mean values of 0.8 and 0.6% for the G102 and G141 grisms, respectively. Figure 5 shows examples for a few selected pixels. Two pixels lying at the mean flat-field response of 1.0 are show in blue and green, as representative of the majority of the pixels. The red points show the wavelength dependence for a 'high' pixel and the magenta points for a 'low' pixel. The open circles show the points generated from the polynomial fit.

Figure 3: Example of the monochromatic image at 10000Å taken with the G102 grism. The mean level is 12330 ADU and the greyscale range ±20% about the mean (black - white).

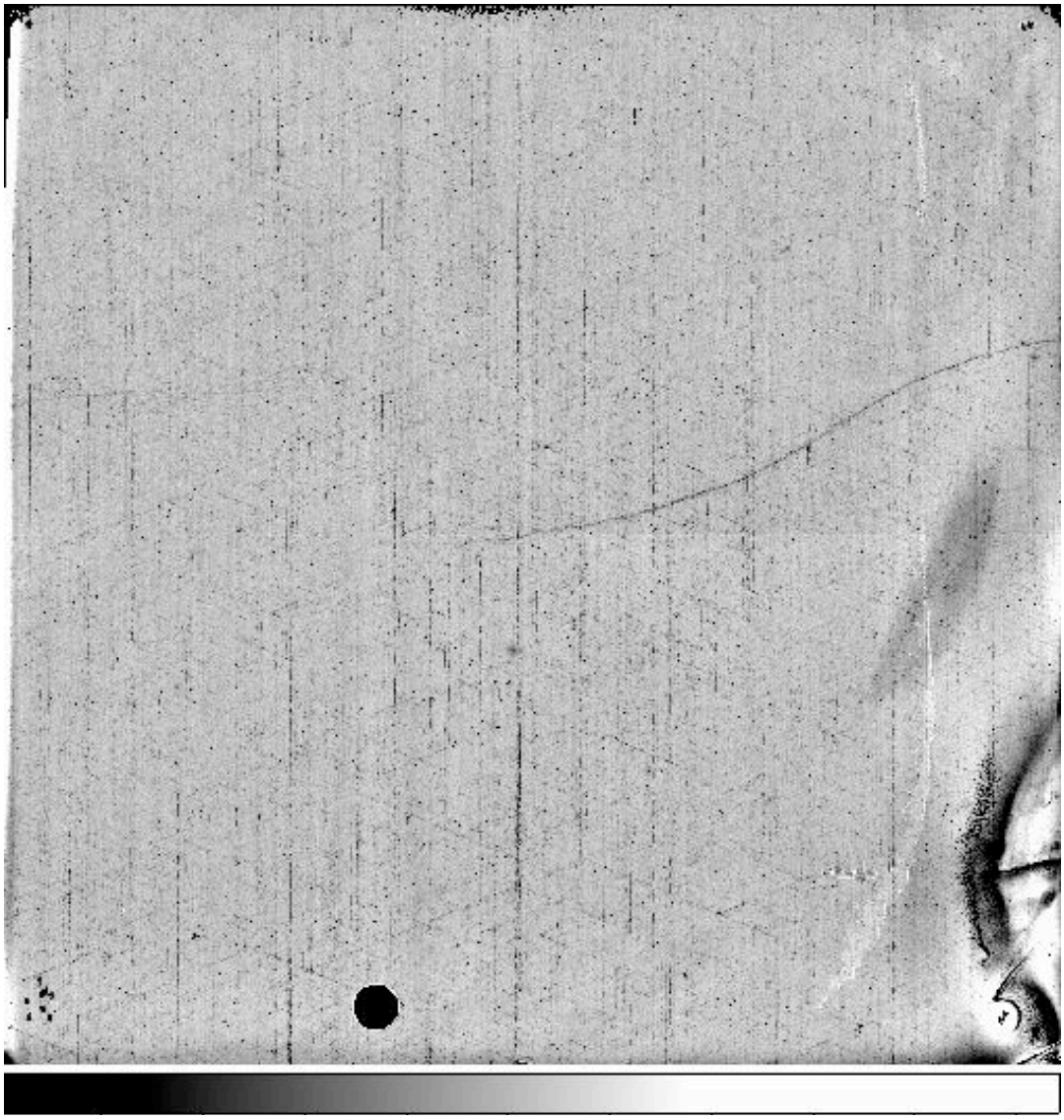

Figure 4: The resulting normalised flat-field image for the G102 grism at 10000Å, derived from the image shown in Figure 3. The greyscale is ±20% about the mean.

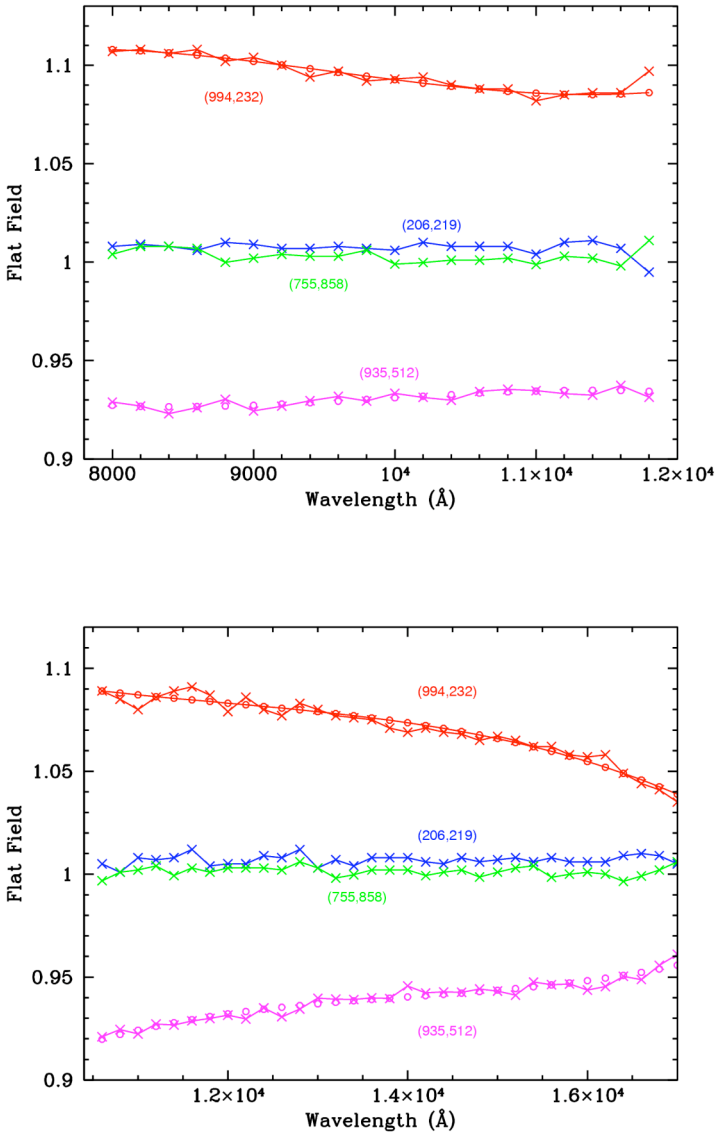

Figure 5: The variation of the flat-field as a function of wavelength for a few selected pixels. Each point refers to the mean value over nine pixels. The upper plot shows the behaviour for the G102 grism and the lower plot for G141. The coordinates of the pixels are indicated. The open circles (for the low pixel (magenta) and high pixel (red) values) are derived from the polynomial fit, which is stored in the flat-field cube.

4. Conclusions

This ISR presented the WFC3 IR grism calibrations carried out during thermal vacuum 3 (TV3; March/April 2008) with the new IR detector (IR4; FPA165). The trace and dispersion solutions derived at one central field position are found to be consistent with the field-dependent solutions derived during TV2. Updated efficiency curves are presented for the G102 and G141 grism modes. Peak efficiency of WFC3 with the G102 and G141 grisms reaches now ~50% and ~55%, respectively. The resulting sensitivity files are used in a simulation package (aXeSIM; Kümmel, Kuntschner, Walsh, 2007) for HST/WFC3 grism observations and are available from ST-ECF Web pages (http://www.stecf.org). Furthermore, we derive up-dated flat-field cubes that provide pixel-to-pixel information as function of wavelength to an accuracy of about 1%.

References

Kümmel, Kuntschner, Walsh, 2007, ST-ECF Newsletter, 43, 8
Kuntschner, Bushouse, Walsh, Kümmel, 2008, ST-ECF Instrument Science Report, WFC3-2008-15